Improving Colloidal Stability of Silica Nanoparticles when Stored in Responsive Gel: Application and Toxicity Study.

Giorgia Giovannini[a], *Paul Warncke*[b], *Dagmar Fischer*[b], *Ondrej Stranik*[c], *Andrew J. Hall*[a], *Vladimir Gubala*[a]*

[a] Medway School of Pharmacy, University of Kent, Chatham Maritime, Kent, ME4 4TB, United Kingdom.

[b] Friedrich-Schiller-University Jena, Institute of Pharmacy, Department of Pharmaceutical Technology, Otto-Schott-Straße 41, 07745 Jena, Germany

[c] Leibniz Institute of Photonic Technology, Albert-Einstein-Straße 9, 07745 Jena, Germany

KEYWORDS nanoparticles, storage, hydrogel, hen' egg test, stability, toxicity, hemotoxicity

ABSTRACT When silica nanoparticles (SiNP) are stored in aqueous solution, even for few hours, they have a tendency to form agglomerates and therefore adapt inhomogeneous structures. Here we present a very practical method to store SiNP in responsive hydrogel. We have confirmed that SiNP kept in the responsive hydrogel do not undergo through undesirable morphological changes and while in storage they maintain their excellent colloidal stability. The effect of SiNP hollowing (i.e. dissolution of the core of the particles that leaves empty cavity inside) was significantly inhibited in the hydrogel, which is a critical feature for any nano-medical applications (e.g. controlled drug release). To demonstrate the applicability of the hydrogel-storing concept within a biologically relevant context, in this work we have evaluated the toxicological effects of the responsive SiNP-gel formulation in a model *in vitro* (human cell line U87GM and hemocompatibility using red blood cells) and *ex ovo* (hen's egg test) experiments. Particles stored in the gel as well as the pure gel did not affect the hemocompatibility (hemolysis and erythrocyte aggregation) up to a concentration of 100 μg/mL. Furthermore, systemic injections into the blood circulation of the chick area vasculosa confirmed the biocompatibility in a more complex biological environment. All evaluated toxicological values (haemorrhage, thrombosis, vascular lysis, and lethality) were comparable with the negative control and no differences in toxicological response could be observed between the SiNP stored in hydrogel and the control nanoparticles stored in the solution.

INTRODUCTION

Functionalized silica nanoparticles (SiNP) are very popular models used in variety of applications and studies ranging from biomedical sensors (Burns et al., 2006, Gubala et al., 2011, Gubala et al., 2010), drug delivery (Ma et al., 2012) and *in vivo* imaging (Ma et al., 2015) among

others. However, their widespread use in commercial products, particularly in nanomedicine, still has not reach the potential that was promised in so many published papers (Venditto et al., 2013). One significant problem that has not been fully addressed so far is the tendency of silica to agglomerate into largely polydispersed clusters or grow (also known as to 'ripen') into large individual particles when they are stored in aqueous solutions (Orts-Gil et al., 2011, Provis et al., 2006). For such reasons, scientists tend to work with 'freshly made' nanoparticles that are not yet agglomerated. This represents a particularly prominent challenge in nanomedical applications, because it is impractical or very often impossible to prepare fresh batch of nanoparticles just before they are to be investigated or used. In addition, the core and/or the surface of SiNP is often physically or chemically altered (e.g. encapsulation of dyes or drugs inside a core-matrix and/or modification of nanoparticle surface with more biocompatible material). The resulting functional SiNP are usually stored for a long time before they are used in the desired biological applications (Nel et al., 2009, Wang et al., 2014). It is not a trivial task to ensure the as-prepared, functionalized SiNP do not undergo through any undesired morphological changes that would affect their toxicity, probability of collision with the target cells, cellular uptake mechanism and retain their intended physico-chemical properties, homogeneous size distribution and function while in storage. Common methods used to stabilize nanoparticles in solution (sterically or electrostatically) include post-synthetic surface modification with polymers such as dextran (Moore et al., 2015), polyethylene glycol (Emoto et al., 1998, Graf et al., 2012, Ruiz et al., 2013, Wang et al., 2015), lipids (Sánchez-Moreno et al., 2015, Zaloga et al., 2015) or by other complex surface chemistry (Fang et al., 2009). Although many of these methods could be sophisticated and elegant, some may still have limits in scalability and practicality. The most common remaining problems are: i) the inadequate stability of silica nanoparticles in buffered, cell culture media

(MacCuspie et al., 2011) and ii) undesired changes in the particle functionality when coated with bulky polymers (Zaloga et al., 2015).

We have previously attempted to improve the colloidal stability of functionalized SiNP by storing them as freeze-dried powders (Moore et al., 2015) but the lyophilisation technique required the use of cryoprotectants, which could be expensive and it could potentially alter the NP's morphology (Kho et al., 2010). More recently, we have reported on a versatile, practical and straightforward approach to store the SiNP in a responsive hydrogel (Giovannini et al., 2017). The SiNP-gel concept is very simple: i) a solution of a highly effective hydrogelator, Fmoc-galactosamine (Fmoc-Gal) is added to nanoparticles; ii) the solution/suspension solidifies into self-supporting hydrogel, thus restricting any undesired phenomena such as particle sedimentation, undesired particle-particle interactions accelerated by Brownian motion (Petersson et al., 2006) and/or effects related to Ostwald ripening of silica nanoparticles (Provis et al., 2006); iii) SiNP are stored in hydrogel for a long time; and iv) when needed, the SiNP-gel formulation is simply shaken by hand, which turns the self-supporting gel into suspension of nanoparticles. Such reconstituted nanoparticles would have the same physico-chemical properties as 'freshly made' nanoparticles. The concept is animated here: https://www.youtube.com/watch?v=EUQns52Q_q4&feature=em-share_video_user.

Such reconstituted SiNP can be used with minimal user manipulation in the desired application. However, when the SiNP-gel formulation was reconstituted into a solution, we noticed the presence of nano-sized gel fibers in the solution. It is therefore critical to understand if the presence of the fibers in the reconstituted SiNP-gel formulation can alter the biocompatibility of the nanomaterial. In this work, we studied the efficiency and applicability of the SiNP-gel formulation in model *in vitro* and *ex ovo* systems. Firstly, transmission electron microscopy (TEM) and

dynamic light scattering (DLS) were used to track the changes in morphology and size distribution of the dextran-coated SiNP (SiNP-Dex) upon longer term storage and when diluted in complex biological media, e.g. cell culture. Secondly, *in vitro* toxicological studies were conducted on the human cell line U87GM (glioblastoma astrocytoma) and hemocompatibility tests on red blood cells were performed to determine whether the SiNP-Dex-gel formulation can induce hemolysis or aggregation of red blood cells when compared with the simple suspension of particles (SiNP-Dex-sol). Additionally, an *ex ovo* test system was used to assess the hemorrhage, thrombosis, vascular lysis and embryonic lethality close to the situation *in vivo* when SiNP-Dex in gel, gel only and SiNP-Dex in solution were injected into the vitelline vein of the chick area vasculosa. All *in vitro* and *ex ovo* assays proved that the proposed gel-storage method is effective in stabilizing silica nanoparticles for long term and the presence of gel or gel debris do not alter the biocompatibility of the nanoparticles. The proposed method is scalable, practical and it can directly be used in biological application without the need for laborious purification steps. Furthermore, we showed that SiNP formulated in gel maintain their morphology even after reconstitution and dilution in complex, biologically relevant media (e.g. cell culture medium).

EXPERIMENTAL

Materials

Cyclohexane (anhydrous, 99.5%), 1-hexanol (anhydrous, ≥99%), Triton® X-100, 3-(Trihydroxysilyl)propyl methylphosphonate, monosodium salt 50 wt % in water (THPMP), (3-aminopropyl)trimethoxysilane [APTMS] (97%), tetraethyl orthosilicate [TEOS] (99,99%), ammonium hydroxide solution (28% w/v in water, ≥99.99%), Fluorescein isothiocyante, Rhodamine B isothiocyanate, dextran from Leuconostoc spp. Mr ~ 40.000, sodium borohydride

(> 99.9%), sodium periodate (> 99.8%), dimethylformamide (DMF) were purchased from Sigma Aldrich. Absolute ethanol, phosphate buffer saline tablets (one tablet dissolved in 200 mL DI water yields 0.01 M phosphate buffer, pH 7.4) were purchased from Fisher Scientific. Hereafter, the use of 'PBS' refers to 0.01 M PBS, pH 7.4. Deionised water was prepared using 200 nm nylon membrane filters purchased from Millipore. Dulcebbo's Modified Eagle Medium (DMEM) without phenol red and pyruvate and a high level of D-Glucose, DMEM with phenol red, antibiotic-antimycotic (containing 10,000 units/mL of penicillin, 10,000 µg/mL of stremptomycin and 25 µg/mL of FungizoneTM) and fetal bovine serum (FBS) were purchased from GibicoTM (Life Technologies). Human glioblastoma cell line (GBM) U87-MG (ATCC® HTB-14™, grade IV WHO classification) was obtained from American Type Culture Collection (ATCC®, Manassas, VA, USA). CellTiter 96® Aqueous One solution cell proliferation assay MTS was purchased from Promega.

Synthetic procedures

SiNP were synthesized according to a well-established reverse-microemulsion method (Bagwe et al., 2004). This procedure yields monodisperse spherical nanoparticles and enables effective encapsulation of fluorescent dyes (Bae et al., 2012).

Synthesis of SiNP – Rhodamine doped nanoparticles

In a dried glass vial, 2 mg of Rhodamine B isothiocyanate (RITC) was dissolved in 2 mL of 1-hexanol and APTMS (5.6 μL) was added. After mixing, the reaction was allowed to proceed for 2 hours under a dinitrogen atmosphere after which time the dye precursor (RITC-conjugated APTMS) was formed.

SiNP were formed in a microemulsion prepared by combining cyclohehexane (7.5 mL), 1-hexanol (1.133 mL), Triton® X-100 (1.894 g), DI water (0.48 mL) in a 30 mL plastic bottle under constant stirring. To this mixture, 100 μL of TEOS was added followed by 0.666 mL dye precursor solution. After 30 min, 40 μL of ammonium hydroxide was added to trigger polymerization. After 24 h stirring, 50 μL of TEOS was added to the microemulsion, followed, after 30 min, by the addition of 40 μL of THPMP whit 5 minute as interval 10 μL of ATPMS. The mixture was stirred for a further 24 h. After that, the microemulsion was broken by adding 30 mL ethanol. The formed SiNP were purified by centrifugation (14000 rpm, 10 min) and re-dispersion in 30 mL ethanol (3 times). After purification, the nanoparticles were stored in ethanol at 4°C.

Synthesis of SiNP – fluorescein doped nanoparticles

Fluorescein loaded SiNP have been synthesized following the same procedure presented above using 2.5 mg of Fluorescein isothiocyante (FITC) instead of RITC for the formation of the dye precursor. The solution of FITC-conjugated APTMS was then added to the microemulsion system during the SiNP synthesis as described above.

Synthesis of SiNP-Dex – Dextran coating

1 μg of 40 kDa dextran was dissolved in 10 mM solution of sodium periodate (0.5 ml) in water at room temperature. After 1.5 hours, the solution was used to re-disperse a pellet of 1 mg of SiNP and the suspension was shaken for 1 hour. 0.5 ml of 10 mM solution of sodium borohydride in DMF was added to the suspension and shaken for another 30 minutes. The samples were then centrifuged (1400 rpm, 10 min) to isolate the particles from the solution and the pellet was washed once with water. The dextran-coated particles were redispersed in water and the suspension was immediately used to prepare both the solution and the gel sample as described in the following paragraph.

SiNP-Dex-gel – Preparation of Nanoparticle-loaded Gels

For a typical nanoparticle-gel preparation, 2 mg/mL solutions of Fmoc-Gal [18] were prepared. The gelator was dissolved in filtered DI water via mechanical stirring at 30°C. Meanwhile, 0.5 mg of nanoparticles was isolated from the water suspension by centrifugation. The pellet was then re-dispersed in 1 mL of gel solution by ultra-sonication for 20 s using the Sonics vibracell probe at 20% amplitude. This sonication step secured the SiNP's maximum monodispersity and also triggered gel formation, which normally occurred in next few minutes. The formation of self-supporting gel could be observed by the naked eye and was confirmed simply by inverting the vial.

SiNP-Dex-sol – Preparation of aqueous SiNP-Dex solutions

Aqueous solutions of SiNP-Dex were prepared following the procedure for NP-Gel samples, but with the omission of Fmoc-Gal.

Characterization

Dynamic light scattering

DLS experiments were performed on the instrument NanoZS ZEN3600 from Malvern Zetasizer with the operating wavelength 633 nm and folded capillary cell (DTS1060) was used with the instrument. All Nanoparticles' dispersions in DI water or DMEM were typically analyzed at concentrations 0.5 mg/mL and at room temperature. Dispersion Technology Software (Zetasizer Nanoseries) was used for the analysis of the data. The default parameter for the water based NP solution were: refractive index: 1.333; viscosity: 0.8872 cP, dielectric constant: 79.5. All values are reported as average of three measurements (n=3) ± SD.

Transmission electron microscopy

TEM micrographs were obtained using a Joel JEM-3200FS transmission electron microscope. Sample preparation involved carefully pipetting the solution of the NP-gel and NP-solution samples in water (approximately 5 μL) onto 'Carbon Films on 400 Mesh Grids Copper' from Agar Scientific. Images were recorded at 250, 200 or 120 kV (accelerating voltage).

Analysis

Processing of Nanoparticle-gels and Nanoparticle-solutions

Prior the TEM and DLS analysis (for nanoparticle samples stored in gels for a specific period of time), the gel was converted to liquid by shaking the sample by hand. The sample was then diluted with water reaching concentration 0.5 mg/mL NPs with total volume of 2 mL. When desired, different concentrations of NPs could be prepared by further dilutions. Solution-stored nanoparticle samples were processed in an identical way to the gel samples.

Analysis of SiNP-Dex-gel and SiNP-Dex-sol diluted in DMEM

Four solution samples and four gel samples of SiNP-Dex were prepared following the procedure mentioned above. After one week of storage, both solution and gel samples were vortexed at maximum speed for 10 s to break the gel matrix, in the case of the gel-samples, and the samples were analyzed with TEM and DLS. All samples were diluted with 1 ml of DMEM. These samples were analyzed after 2, 4, 6 and 8 hours, respectively, using DLS, TEM and by tracking their flow in a microfluidic chip after further dilution with filtered DI to 0.125 mg/mL of NPs.

Toxicology protocols

MTS assay

The human cell line GBM cell line U87-MG (ATCC® HTB-14™ , grade IV WHO classification) was cultured in monolayer in a flask. U87MG cells were maintained in DMEM supplemented with

FBS 10%, antibiotic 1% and sodium pyruvate 1%. Cells were kept at 37°C in a humidified atmosphere containing 5 % CO_2. To evaluate the toxicity of SiNP stored in solution and in gel, cells were seeded into 96-well plate at a density of 8000 cells/well and allowed to adhere for 24 hours. SiNP samples were then diluted to appropriate concentrations with medium and immediately applied to the cells from which the old medium was removed. A preliminary study to determine the influence of the incubation time was accomplished. Cells were incubated for different times (2, 4, 8 and 12 hours) with 50 µg/mL of each sample. Once the incubation time was defined, the cells viability was evaluated treating cells with different concentrations of samples. SiNP concentrations of 100, 50 and 25 μg/mL, respectively, were incubated with cells for 2 hours to evaluate the dose/survival conditions. After incubation, the samples were carefully removed from the wells and 100 µL of fresh medium were added and, after addition of 20 µL of MTS reagent, the plate was incubated for another two hours. Healthy cells produce metabolic enzymes that modify MTS reagent. The product adsorbs at 490 nm therefore the intensity of the signal measured at this wavelength indicates cell viability. The latter experiment has been accomplished in triplicates. Untreated cells were used as control and the value measured represented the 100% of cell viability. The absorbance at 490 nm of SiNP-Dex-sol SiNP-Dex-gel and gel alone in absence of cells were used as blank.

In vitro hemocompatibility test

To predict the hemocompatibility of the synthesized particles, the hemolytic activity and the aggregation of erythrocytes were determined using *in vitro* red blood cell (RBC) assays according to Bauer et al. (Bauer et al., 2012). Briefly, heparinized sheep blood samples were purified and washed several times by centrifugation (2800×*g*, 7 min, 3 times) to remove the plasma and to collect the red blood cells. The washing steps were performed with an isotonic 5% glucose solution

buffered with 10 mM 4-(2-hydroxyethyl)-1-piperazineethanesulfonic acid (GlcHEPES) adjusted to pH 7.4.

To analyze the red blood cell aggregation after interaction with the samples, the red blood cell stock solution was adjusted to 20.000 erythrocytes/µL in GlcHEPES solution. The dextran coated SiNP (either RITC- or FITC-labeled) in gel or solution as well as the gel (pure) were stored in a stock solution of 1 mg/mL and diluted with DI water to the test concentrations. Samples were pipetted in a 96*well*-plate and mixed with the red blood cells to the final concentrations 3.125, 6.25, 12.5, 25, 50 and 100 µg/mL. Gel samples were liquefied using a vortex and diluted afterwards. The mixture of erythrocytes and samples was incubated for 2 h at 37°C in an incubator (WTC Binder Tüttlingen, Germany) under continuous shaking (1350 rpm). After incubation, the plates were analyzed by light microscopy (Primovert, Carl Zeiss, Jena, Germany) and by spectrophotometric measurements at 645 nm (Tecan Spark 10 M, Crailsheim, Germany) to quantify the RBC aggregation. As positive control a poly(ethylene imine) coated nanoparticle (fluidMAG-PEI 750/O, chemicell GmbH, Berlin, Germany, 160 µg/mL) was used, since this type of particle was proven to cause significant aggregations due to its positive surface charge(Schlenk et al., 2017). The negative control (GlcHEPES with erythrocytes), the blank (GlcHEPES without erythrocytes) and the sample controls (samples without erythrocytes) were used in each experiment. To quantify the erythrocyte aggregation, ΔAbs was calculated from the absorbance at 645 nm using the following equation according to Schlenk et al.(Schlenk et al., 2017):

$$\Delta\mathrm{Abs} = \left(Abs_{negative\ control} - Abs_{blank}\right) - \left(Abs_{sample} - Abs_{sample\ control}\right) \quad (1)$$

Light emitted through the RBCs in suspension is scattered by the erythrocytes. Non-aggregating samples are characterized by a lower amount of light reaching the detector (increased absorption). Therefore, test solutions with considerably lower absorbance values compared to the negative

control were regarded as RBC aggregation and resulted in increased ΔAbs values. Qualitative evaluation of aggregation by light microscopy was grouped into 3 stages: At stage 1 no aggregation was detectable and all erythrocytes stayed discrete in suspension; stage 2 indicated moderate aggregation with rouleaux formation, but the majority of the erythrocytes were still discrete in suspension; in stage 3 almost all erythrocytes were aggregated to big clusters and no free cells remained discrete in suspension.

The hemolytic activity of the samples was analyzed by the quantification of the released hemoglobin by spectrophotometric measurement. The red blood cell stock solution was adjusted to 1.800.000 cells/µL and mixed (1:1) with the samples to the final test concentrations 3.125, 6.25, 12.5, 25, 50 and 100 µg/mL. After 60 min incubation at 37 °C under continuous shaking (450 rpm), the red blood cells were removed by centrifugation at 2250×*g* (Eppendorf Centrifuge 5804R, Eppendorf AG, Hamburg, Germany) and the supernatant was spectrophotometrically quantified at 544 nm. Blank values were determined measuring only the GlcHEPES solution without cells. Particle test samples diluted with GlcHEPES were tested in similar concentrations without erythrocytes (sample control) in order to exclude any influence on the absorption measurement. Cells treated with 1% solution of the nonionic surfactant Triton X-100 (Ferak Berlin GmbH, Berlin, Germany) was used as positive control. Untreated cells served as negative control. The percentage of the released hemoglobin in relation to the positive control was determined using following equation:

$$Hemolysis\ [\%] = \frac{(Abs_{sample} - Abs_{sample\ control}) - (Abs_{negative\ control} - Abs_{blank})}{(Abs_{positive\ control} - Abs_{blank})} \times 100 \qquad (2)$$

According to the ASTM F756-00 standard, the hemolytic activity of the samples was classified as 0-2% non-hemolytic, 2-5% slightly hemolytic or >5% for hemolytic activity. Experiments were run in triplicates and performed with dextran coated particles (either RITC or FITC labelled

particles with similar size and surface potential) stored in solution or gel as well as with the pure gel. Data of the RBC aggregation and hemolysis assay are represented as mean ± SD.

Ex ovo hen's egg test on chick area vasculosa (HET-CAV)

To investigate the effect of the particles in a dynamic complex biological test system, we used a shell less hen's egg test on the chick area vasculosa (HET-CAV) according to Schlenk et al. (Schlenk et al., 2017). Briefly, fertilized eggs were incubated for 72 h at 37 °C. After incubation, eggs were transferred into petri dishes (Greiner Bio-One GmbH, Frickenhausen, Germany) containing Ringer's solution pH 7.0 and incubated for further 24 h. For the experiments only eggs with a well-developed chick area vasculosa according to Hamburger and Hamilton stages 14-17 were selected (Hamburger et al., 1951). Test samples (SiNP-Dex-sol, SiNP-Dex-gel and gel alone) were stored in a stock solution of 1 mg/mL and diluted to the test concentration (50 or 125 µg/mL) with DI water. The gel samples were liquefied by mechanical shaking using a vortex and diluted equally to the final test concentrations. A volume of 2 µL of each sample was injected into the upper or lower vitelline vein of the embryos chick area vasculosa (CAV) using a micro injector (Sutter Instrument Company, Novato, USA). According to the recommendations of the Interagency Coordinating Committee on the Validation of Alternative Method (ICCVAM) for the HET-CAM test 0.9% sodium chloride was used as negative control. Since samples were diluted with DI water it was run as solvent control in each experiment. As a positive control a solution of branched poly(ethylene imine) (25 kDa, 25 mg/mL, kindly provided by BASF, Ludwigshafen, Germany) was used. Each sample was tested at least in two independent experiments with a minimum total number of 8 eggs. Eggs were analyzed after 0, 1, 2, 4, 8 and 24 h for thrombosis, hemorrhage, vascular lysis or embryonic lethality.

RESULTS AND DISCUSSION

NPs synthesis and storage-stability analysis by TEM and DLS

Pristine SiNP loaded with Rhodamine B (for imaging purposes and to assess the possible 'drug' leaching effect) were prepared following a well-known reverse microemulsion protocol (Bagwe et al., 2004). Such SiNP usually displays a negative surface charge, which is imparted by the use of a mixture of organosilanes (THPMP:APTMS in 4:1 ratio v/v) to form an outer shell, usually few nanometres thick. According to DLS analysis, the average size of the SiNP was 157 nm (surface charge -32.4 mV), while the same sample by TEM analysis gave average size of 59 nm. This discrepancy in size is understandable as DLS allows to observe the full hydrodynamic radius of nanoparticles in their solvated state, whereas TEM measures the same sample in the dry state (i.e. the most compact state) (Cascio et al., 2014, Sokolov et al., 2015). The presence of $-NH_2$ groups on the surface of SiNP (from APTMS) allowed coating with polyaldehyde dextran (40kDa) using a procedure published in our group previously (Moore at al., 2015). The reaction is schematically depicted in Figure 1a. The reasons for dextran coating were two-fold: i) dextran is a well-known biocompatible polymer used to coat nanoparticles applied in the clinics (Peng et al., 2015, Shaterabadi et al., 2017) and ii) dextran-coated SiNP can be readily functionalized with biomolecules such as antibodies to provide SiNP with cell-targeting capabilities (Tivnan et al., 2012). The fact that dextran was successfully grafted onto the SiNP surface was evident from both the DLS and TEM data (Table 1) and is in agreement with previously published data (Moore et al.

2015). The size of SiNP-Dex was 160.2 by DLS and 63 nm by TEM. Importantly, the zeta potential, indicative of the overall surface charge of the measured colloid decreased from -32.4 to -25.1 mV, when compared with the pristine SiNP, suggesting a successful chemical reaction on the nanoparticle surface.

Table 1 Comparison of size and polydispersity of the SiNP prepared by the microemulsion method measured by DLS and TEM in water at a concentration of 0.25 mg/mL. Measurements are reported as average values (n=3) ± SD.

	DLS			TEM
	Ø (nm)	PDI	ζ (mV)	Ø (nm)
SiNP	157.0 ± 48.2	0.277	-32.4 ± 0.87	59 ± 16
SiNP-Dex	160.2 ± 29.7	0.287	-25.1 ± 0.55	63 ± 11
SiNP-Dex-sol (1week)	133.0 ± 42.3	0.238	-27.5 ± 1.84	109 ± 19
SiNP-Dex-gel (1week)	126.1 ± 21.2	0.354	-11.5 ± 2.24	91 ± 28

It is noteworthy to mention that DLS is a highly accurate technique when used with samples of narrow particle size distributions especially in the range of 2–500 nm (Tomaszewska et al., 2013). Polydispersed samples or any samples with additives that can potentially scatter light (e.g. the nano-sized gel fibres remaining in the solution after storage) can distort the results and limit the use of DLS to accurately assess the degree of SiNP agglomeration while in a solution and in a hydrogel. When the SiNP-gels were stored and then 'converted' into a solution (by shaking), the DLS measurements provided inconclusive data because of the scattering contribution of the gel fibres present in the solution. Therefore, we have analysed the changes in morphology and the evolution of agglomerates or other higher ordered species for both SiNP stored in solution and in hydrogel (SiNP-Dex-sol and SiNP-Dex-gel respectively) by TEM. Unlike DLS technique, TEM allows for direct visualization of the nanoparticles even in the presence of other debris or

nanofibres, making it possible to identify the presence of different populations of particles and other entities in the sample.

In the first experiment, one set of SiNP-Dex was stored in water (SiNP-Dex-sol) while another identical set of SiNP-Dex was stored in a hydrogel (SiNP-Dex-gel). After 7 days of storage at 4°C in the dark, both samples were analysed by TEM. The SiNP-Dex-sol sample was deposited directly on the TEM grid as removed from the refrigerator, the SiNP-Dex-gel sample was shaken by hand to 'break' the hydrogel into a solution before deposited on the TEM grid. The images, shown on Figure 1c indicate that both nanoparticle samples were relatively stable although the diameter of the SiNP-Dex-sol was slightly higher when compared to SiNP-Dex-gel. Interestingly, upon careful analysis of the TEM images, we noticed the SiNP-Dex-sol hollowing, a phenomenon described previously in the literature (Gubala et al., 2010, Moore et al., 2017, Park et al., 2009, Rimer et al., 2007). For example, Park *et al.,* O'Connell *et al*. and also Moore *et al*. reported on the degradation of silica NPs into hollowed spheres due to etching under basic, aqueous conditions (O'Connell et al., 2017, Park et al., 2008). The dissolution and hollowing of silica matrix are highly unwelcome effects, especially when SiNP are designed as vehicles to be encapsulated with drugs as nano-drug delivery system or with contrast agents (e.g. fluorescence, MRI or luminescence) for *in vivo* imaging applications. Importantly, the nanoparticle degradation effect was negligible for SiNP-Dex-gel after 1 week of storage as noticeable from the TEM images in Figure 1. Therefore, SiNP-Dex-gel will presumably retain their cargo for much longer period of time when compared to the same nanoparticles stored in solution.

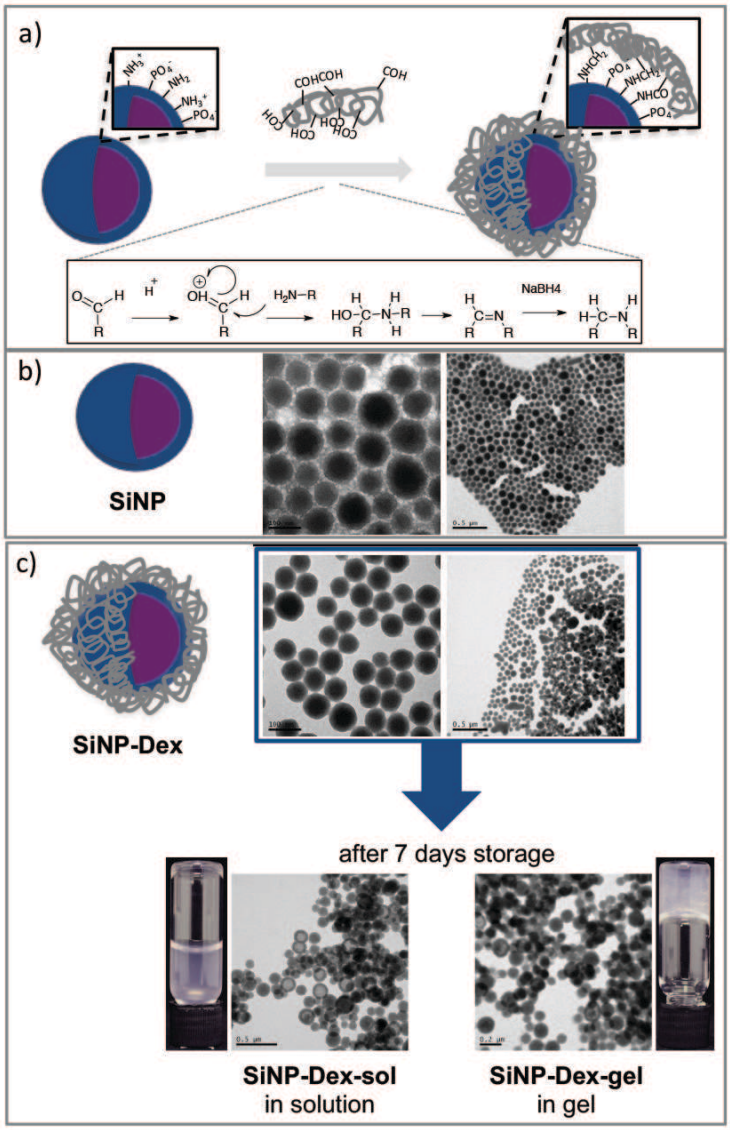

Figure 1 (a) schematic illustration of the SiNP surface composition and the reaction with polyaldehyde dextran to form SiNP-Dex; the inset shows the mechanism of *Schiff base* formation and subsequently stabilisation of the C-N bond by $NaBH_4$ reduction (b) TEM images of the SiNP and (c) TEM images of the SiNP-Dex and also SiNP-Dex-sol and SiNP-Dex-gel after 1 week of storage at 4˚C in the dark.

The hollowing effect was further probed qualitatively in a more complex biologically relevant medium. SiNP-Dex-sol and SiNP-Dex-gel were stored for 1 week and then diluted to 0.25 mg/mL

in Dulbecco's Modified Eagle's Medium (DMEM). We have previously reported on the challenges to maintain good colloidal stability of SiNP in enriched culture media (Moore et al. 2015). The hollowing/dissolution effect, the possible changes in the nanoparticle morphology and the degree of aggregation of nanoparticles were assessed by TEM for both SiNP-Dex-sol and SiNP-Dex-gel. Both solution and gel samples after storage were diluted with DMEM and placed at 4°C for 8 hours. This experiment was designed to reproduce a possible real-life scenario were SiNP were first synthesised, then stored and finally reconstituted to be used in a model biological experiment. After 2, 4, 6 and 8 hours in DMEM at 4°C the samples were analysed by TEM (Figure 2). For both samples, the dissolution of the silica matrix is already partially evident after 2 hours. However, the hollowing effect, 'bridging' of individual particles and the evolution of the nanoparticles into larger agglomerates or even an undefined polymer matrix that would no longer fit to definition of nanoparticle is arguably accelerated with SiNP-Dex-sol. The SiNP-Dex-gel also experienced hollowing and dissolution but, after 8 hours in DMEM, it is still possible to recognize individual nanoparticles, albeit with a wider size distribution than at the beginning of the experiment (time = 0h).

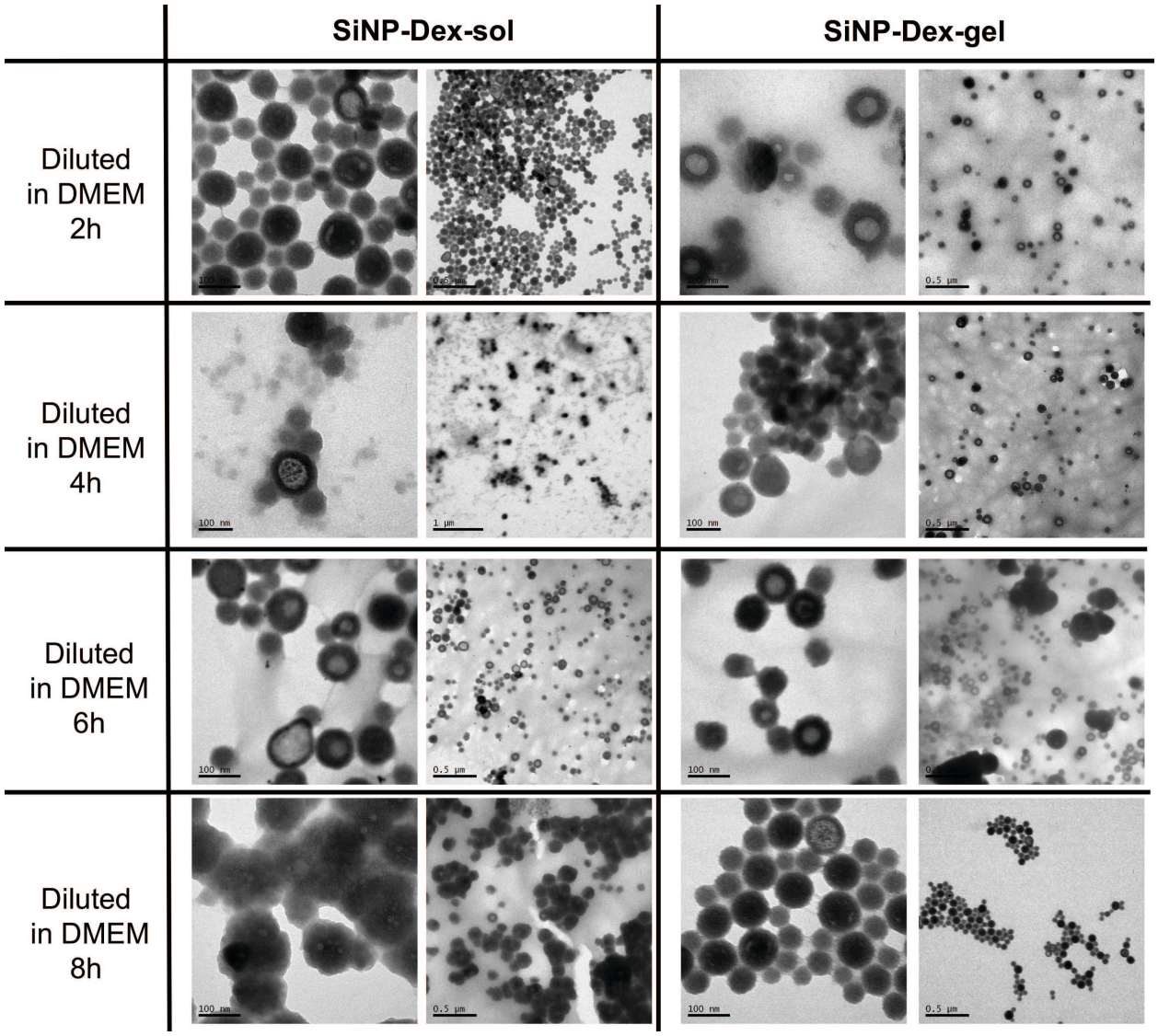

Figure 2 TEM images of SiNP-Dex-sol and SiNP-Dex-gel while incubated in DMEM for up to 8 hours.

In vitro microfluidic flow assessment

Dye-doped SiNP and drug-encapsulated SiNP have been reported to play major roles either as bright labels in biomedical diagnostics (Bae et al., 2012) or as drug carriers in nano-drug delivery systems (NDDS) (Tivnan et al., 2012). The successful outcome in both applications depends strongly on the good colloidal stability and homogeneous distribution of the nanoparticles that are

usually placed in buffered solutions or more complex biological media, such as serum, plasma or whole blood. When SiNP are used *in vivo* as NDDS, agglomeration of SiNP is a highly undesired effect as it often leads to premature clearance of the material from the bloodstream and its accumulation in the liver or lungs(Ruiz et al., 2013). We have therefore designed a simple qualitative test to visually compare the degree of agglomeration between SiNP-Dex-sol and SiNP-Dex-gel in a model microfluidic chip. Since the SiNP were labelled with a fluorescent dye (Rhodamine), it was possible to image the flow of the nanoparticles by epifluorescence microscopy (Axio Imaginer A1.m Zeiss, 10 x Objective, Filter set – 77HE from Zeiss, PCO camera). Both SiNP-Dex-sol and SiNP-Dex-gel were used in this test after 1 week of storage. The SiNP-Dex-gel were reconstituted into solution prior the injection into the microfluidic chip, which featured the zig-zag shaped microchannel (geometrical parameters of the channel: width = 150 μm, depth = 40 μm). The two solutions (i.e. SiNP-Dex-sol and reconstituted SiNP-Dex-gel, both diluted in DMEM) were slowly pumped through this channel after 2, 4, 6 and 8 hours of the dilution with the medium while the fluorescence images were recorded (Figure 3). A short video was also recorded and it is available here (https://www.youtube.com/watch?v=EmAzEVbGbGE&feature=em-share_video_user).

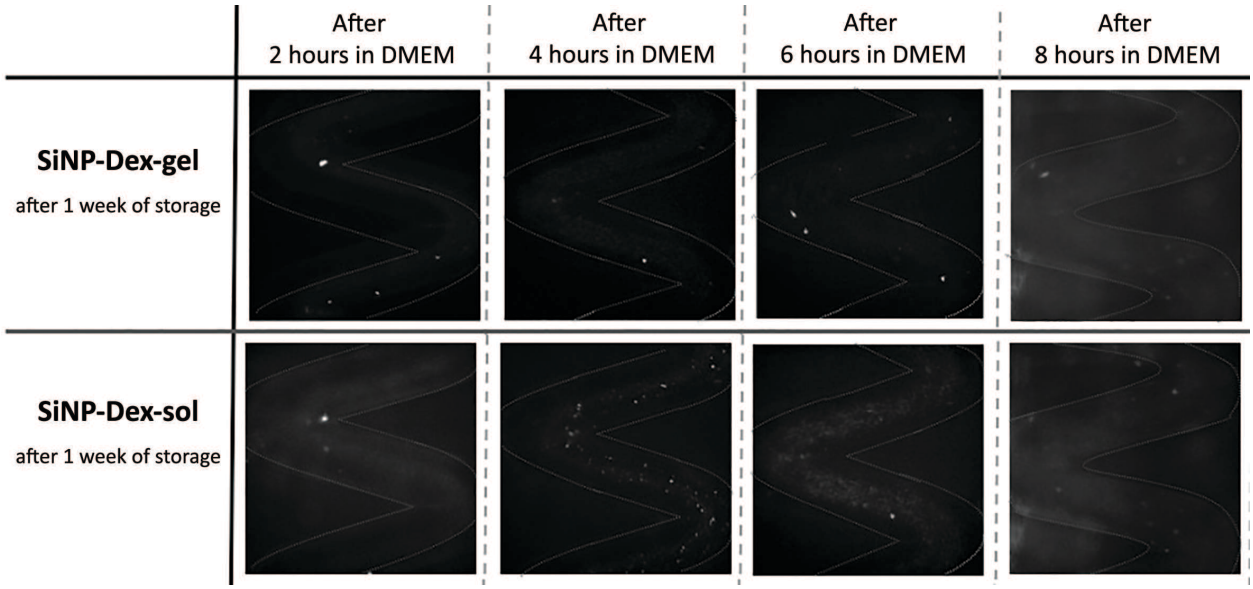

Figure 3 Microscope images of SiNP-Dex-sol and SiNP-Dex-gel samples diluted in DMEM at different time point while they were flowing through the microfluidic chip. The particles were analyzed at concentration of 0.125 mg/mL and samples were pumped through the channel at a flow rate of 0.3 μL/s. More agglomerates were noticeable in SiNP-Dex-sol.

It is important to mention that, due to the size of the original particles and the camera resolution, it was impossible to observe the individual nanoparticles. It was, however, possible to identify very clearly any agglomerates (the smallest fluorescent agglomerates detectable by this method were 4.5 μm in diameter). SiNP-Dex-gel, reconstituted in DMEM, showed the occasional agglomerate flowing through the channel within the 8 hours of being in a DMEM solution. This was in stark contrast with the solution of SiNP-Dex-sol in DMEM, which showed a significant number of visible objects (i.e. agglomerates or aggregates, not nano-sized anymore) flowing through the channel already at 4h. We have attempted to obtain more quantitative analysis of the degree of aggregation/agglomeration for each formulation. However, due to the nanoparticle hollowing effect over time and the associated dye leaching for SiNP-Dex-sol, we were only able to approximately quantify the colloidal stability of both SiNP-Dex-sol and SiNP-Dex-gel,

providing an indication of their behaviour while flowing in a microchannel. We have analyzed the fluorescent intensity values measured in the channel for each sample at 2, 4, 6 and 8 hours' time points. Although this can only provide some quantitative indication of the nanoparticle agglomeration/aggregation, we observed between 1.7 – 3.4 times more agglomerates/aggregates in the SiNP-Dex-sol at every time point as compared to the SiNP-Dex-gel sample.

Toxicological studies

The hallmark of the presented SiNP storage method is the option of storing the nanomaterial inside a hydrogel, thus preserving its carefully designed properties and unique function. When needed, the particles can be brought back in suspension simply by shaking. After appropriate dilution, the sample can be used directly in any desired application. However, the reconstituted solution may contain fibre debris (i.e. higher-order assemblies created by the Fmoc-Gal hydrogelator). As shown in Figure 4, partial or complete dissolution of the Fmoc-gal fibres can be achieved by diluting the 'broken' hydrogel sample. The complete dissolution of the gel fibres is also proportional to the amount of the aqueous medium (i.e. correlates with the dilution ratio) and it can be accelerated in solvents containing ethanol.

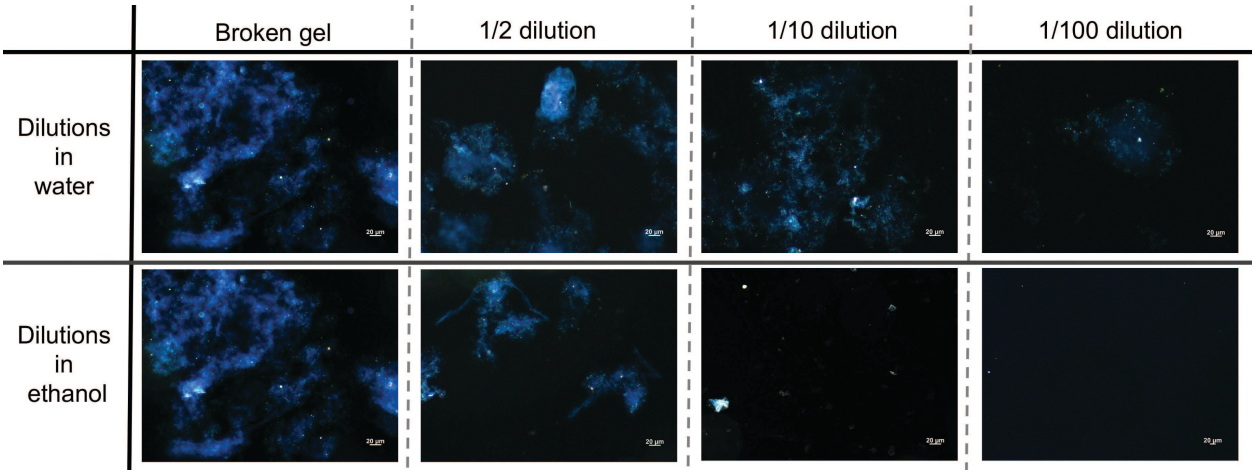

Figure 4 Dissolution of the gel fibres (blue scattering) of Fmoc-Gal (2 mg/mL) after 1/2; 1/10; and 1/100 dilutions in water and absolute ethanol.

Because of the potential presence of the gel fibres, we addressed the need of proving that these residues in the SiNP-Dex-gel sample do not alter the effect of the nanomaterial when exposed to biological systems. We have designed simple *in vitro* and *ex ovo* assays in order to determine the effects of the gel and its components on the toxicity of SiNP-Dex.

a) MTS assay

In the first instance, we obtained basic cytotoxicity data from an MTS assay performed with a human glioblastoma astrocytoma hematopoietic cell line (U87MG), mixed and incubated with three formulations: SiNP-Dex-gel, SiNP-Dex-sol and hydrogel without nanoparticles (all gels were reconstituted into solutions before the MTS assay). The U87MG cell line is known to be studied in experiments involving nanomaterials (Alkilany et al., 2010, Gianoncelli et al., 2013). The fact that they adhered to surfaces allowed us to remove the analysed sample after incubation, thus limiting any possible interferences between the particles/gel and the MTS reagent (tetrazolium salt). A preliminary experiment to determine the incubation time was performed, in which all samples at the concentration of 50 μg/mL were incubated with cells and the viability was tested

after 2, 4, 8 and 12 hours (data not showed). No relevant difference in cell viability was noticed between the different time-points, therefore 2 hours of incubation was used in the MTS experiments. All formulations were incubated for 2 hours at different concentrations (100, 50 and 25 μg/mL) with U87MG cells in a 96-well plate format in cell culture medium (in triplicate). Cells alone were used as a control and the absorbance measured after MTS reagent addition was regarded as 100% of cell viability. The MTS assay results are summarised in Figure 5A. After two hours of incubation, negligible cytotoxicity was detected with all studied samples at the lower concentrations, but a small drop in cell viability was observed at the high end of the concentration range for SiNP-Dex-gel or Gel alone.

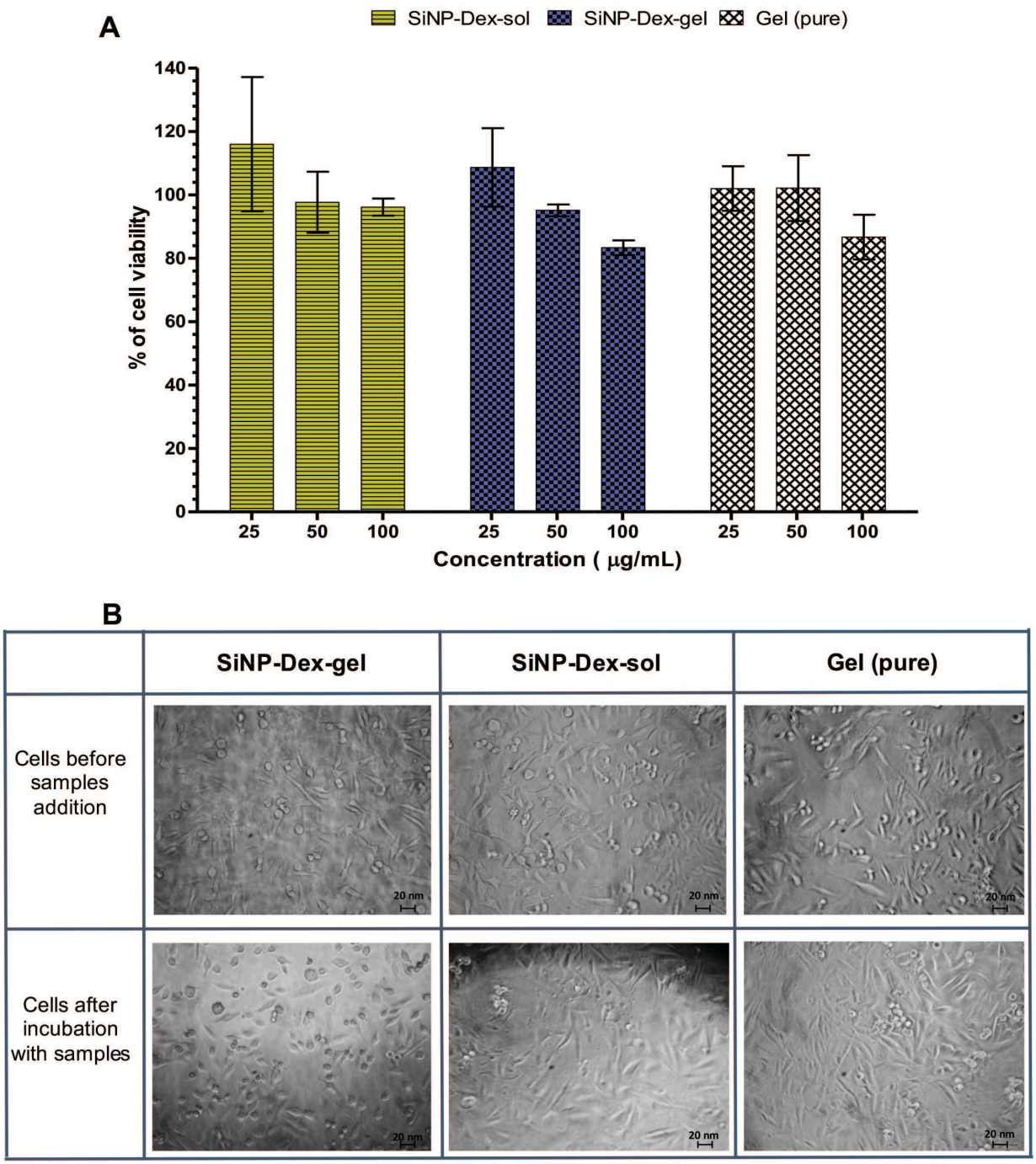

Figure 5 MTS assay data on U87MG cell line: A) Cell viability as a function of different concentrations (100, 50 and 25 μg/mL) over the period of 2 hours. B) Evaluation of cell morphology during MTS assay. No relevant difference in the morphology of glioblastoma cells is noticeable.

In addition to the MTS assay, we have qualitatively investigated the cell morphology before and after incubation with all samples (Figure 5B). No significant changes in the cell morphology were observed, even when treated with the highest concentration of the nanomaterial. The cells appear spherical at lower degrees of confluence and more "star-like/branch out" at higher degrees of confluence.

b) Hemocompatibility testing

Blood is composed of a multitude of cell types, ranging from simple oxygen-carrying erythrocytes to sophisticated antigen-specific lymphocytes. The various cells participate in a vast array of functions, including tissue repair and immune responses as well as oxygen transport. After the systemic injection of the particles they can interact with blood components such as red blood cells (RBCs) as the major component of the blood cell pool possibly causes severe aggregation and hemolysis. Therefore, we tested the interactions of SiNP-Dex-sol and SiNP-Dex-gel as well as the pure gel (after the gel samples were liquefied) with isolated RBCs *in vitro*. In this experiment, samples of SiNPs with either a positively charged Rhodamine B isothiocyanate (RITC) or a negatively charged Fluorescein isothiocyanate (FITC) were prepared to provide an insight into the effect of the encapsulated material on the hemolysis. Hemolytic behavior would demonstrate a possible damage of the erythrocytes membrane accompanied by the release of hemoglobin that was measured by the absorbance of the RBC suspension and classified according to the ASTM F756-08 standard. As shown in Figure 6A, up to a concentration of 100 μg/mL, neither SiNP-Dex-sol, SiNP-Dex-gel (RITC or FITC doped) nor the gel (pure) showed hemolytic reactions (hemolysis < 2%) with the red blood cells in comparison to the positive control (1% Triton-X-100, 100% value).

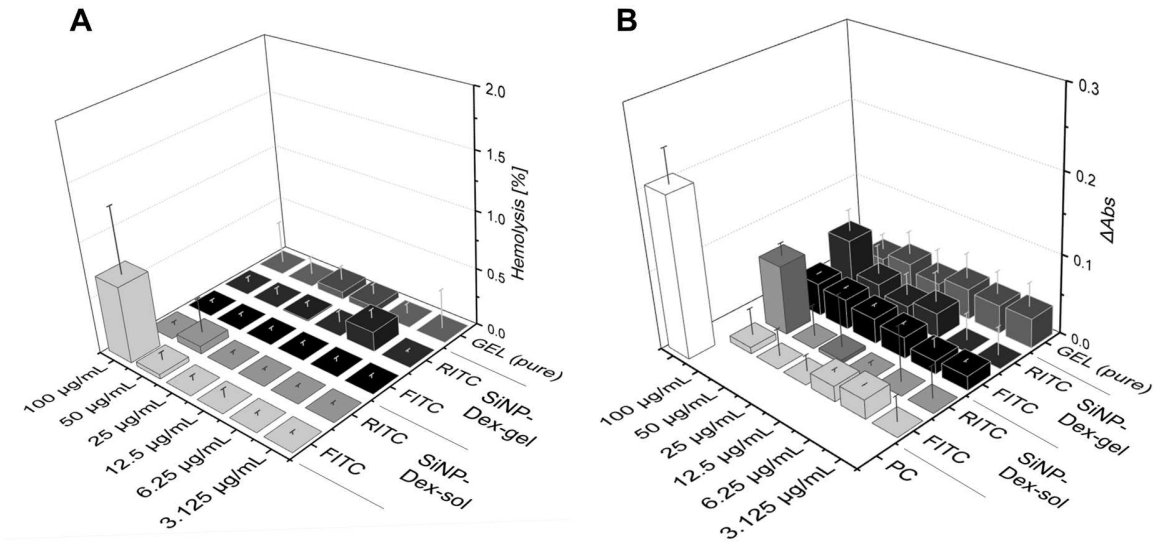

Figure 6: Hemocompatibility testing: A) Different tested nanoparticle samples and gel showed no hemolysis (< 2%) in all tested concentrations up to 100 µg/mL; B) All tested samples showed lower ΔAbs values representing RBC aggregation compared to the positive control (PC) up to 100 µg/mL. Data are presented as mean ± SD.

Besides hemolysis, RBC aggregation could cause toxic reactions after the systemic injection of particles leading to circulatory side effects or toxic reactions. After the mechanical reconstitution of the gel, RBC aggregation was investigated regarding the influence of different storage conditions (sol or gel) for particles as well as to determine the hemocompatibility of the pure gel after liquefaction. Therefore, we investigated the aggregation of isolated erythrocytes after incubation with the samples by absorbance measurements at 645 nm and by light microscopy. The ΔAbs values were calculated to determine the aggregation quantitatively. Due to the aggregation of almost all erythrocytes in clusters (stage 3), the positive control (PC) showed the highest ΔAbs value (0.204 ± 0.042) of all samples. The samples themselves did not interact with the absorbance

measurement (data not shown). The SiNP-Dex-gel, SiNP-Dex-sol as well as the pure gel showed no aggregation up to a concentration of 50 µg/mL (ΔAbs-values < 0.05, Figure 6B). However, at a concentration of 100 µg/mL an influence of the dye could be observed. Whereas the RITC as well as the FITC-loaded SiNPs-Dex-gel (RITC: ΔAbs = 0.075 ± 0.028, FITC: ΔAbs = 0.042 ± 0.001) and the pure gel (ΔAbs = 0.058 ± 0.025) caused no RBC aggregation (stage 1) in a concentration of 100 µg/mL, SiNP-Dex-sol particles loaded with RITC caused moderate aggregations (stage 2-3) accompanied by slightly increased ΔAbs values (ΔAbs = 0.088 ± 0.016). Since this was not observed for the FITC-loaded SiNP-Dex-sol (stage 1, ΔAbs = 0.008 ± 0.035) at this concentration, this effect could be attributed to the release of the positively charged RITC during the storage in solution. Therefore, RITC (pure) was tested for RBC aggregation in similar concentrations to confirm the interactions with erythrocytes (data not shown). Due to the fact that no differences regarding the aggregation for RITC- or FITC-loaded particles stored in the gel (stage 1) were observed by light microscopy, it was indicative of a delayed release of substances entrapped into the SiNPs. In conclusion, the gel did not affect the hemocompatibility of the particles *in vitro*. Particles stored in the gel as well as the pure gel did not cause hemolysis or RBC aggregation up to a concentration of 100 µg/mL.

c) Hen's egg test on the chick area vasculosa *ex ovo*

For further investigations regarding the toxicity of the reconstituted gel, the hen's egg model was used as a more complex biological system to evaluate the effect of the NPs and the gel close to the situation *in vivo*. The assessment of the toxicological profile of particles close to the situation *in vivo* is a crucial point in the evaluation of the biocompatibility. Therefore, we used a chicken egg based test system in the earliest stages of the development to test the reactions after the systemic injection of the SiNP-Dex-sol, SiNP-Dex-gel and the gel (pure) samples in two different

concentrations (50 and 125 µg/mL). The HET-CAV offers a vascularized membrane close to the situation *in vivo* (Müller et al., 2015). Changes of the vascularized membrane due to toxic reactions (hemorrhage, thrombosis, vascular lysis) or embryonic lethality were investigated after the intravenous injection of particles (FITC-loaded) or the gel (pure) for up to 24 hours. The data of two independent experiments are represented in Figure 7. The negative control (0.9% sodium chloride) as well as the solvent control (DI water) caused negligible hemorrhagic events (1/11 eggs) that could be related to the injection itself and correlated with the historic lab values (hemorrhagic events in 0-1/10 eggs). This is the same for the solvent control, where 1/10 embryo died after 24 h as well as the negative control with occasional hemorrhagic effects (0-1/10 eggs) and embryonic lethality after 24 h (0-1/10 eggs). In comparison, the injection of the positive control (branched PEI 25 kDa, 25 mg/mL in DI water) strongly induced thrombotic events (directly after injection) that caused lethality in all eggs (11/11) after 1 h.

The test samples induced mild and reversible hemorrhagic events after the injection comparable to the control groups (1 egg per group). Embryonic lethality occurred occasionally in both concentrations of SiNP-Dex-sol (1/10 eggs for 50 µg/mL and 1/12 eggs for 125 µg/mL), in the lower concentration of SiNP-Dex-gel (1/10 eggs at 50 µg/mL) and after injection of the higher concentration of the gel (1/10 eggs for 125 µg/mL). The slight hemorrhagic effect as well as the sporadic appearance of embryonic lethality after 24 h also appeared in the control groups and were suggested as non-specific related to the biological variability. Further, these data were comparable to our lab historical data as described above. No significant differences regarding the toxicity between the test concentrations 50 µg/mL and 125 µg/mL were observed. In conclusion, particles stored in gel as well as the pure gel caused no toxic reactions after the systemic injection in the chick area vasculosa model. Therefore, the gel and tested particles could be considered as

biocompatible in the tested concentrations. *In vitro* and *ex ovo* experiments indicated the suitability of storing SiNPs within a gel matrix as a non-toxic alternative.

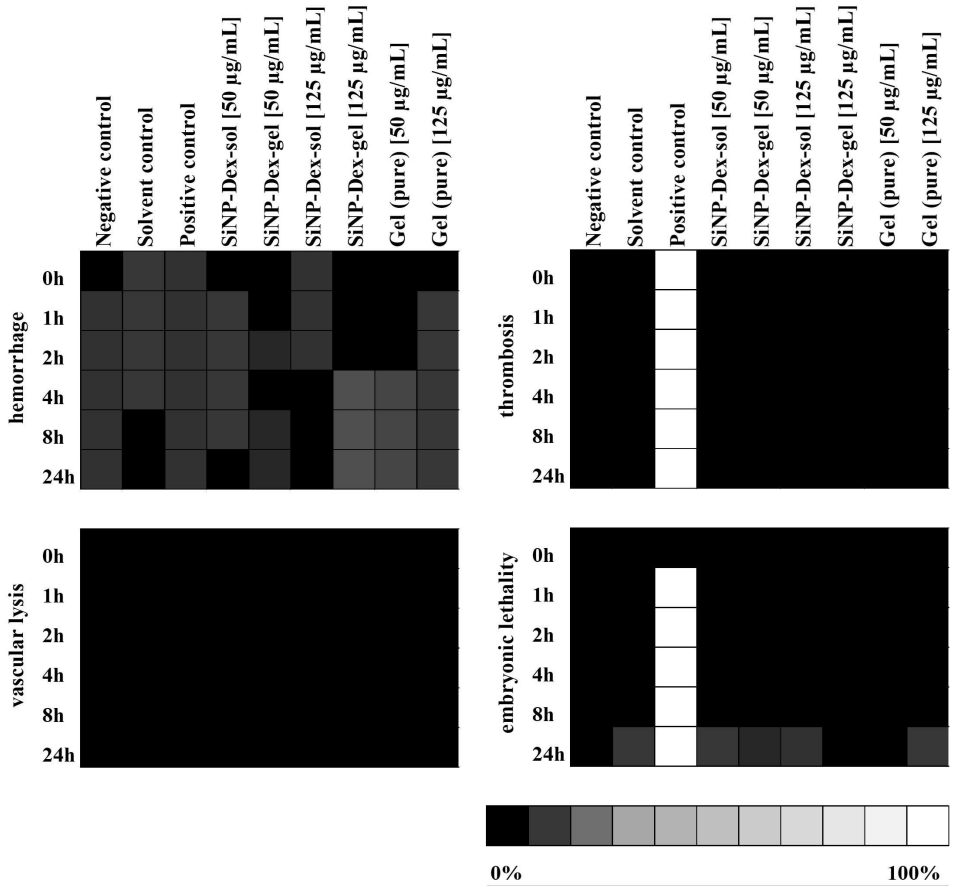

Figure 7 Clustergram showing the time-dependent toxic effects of intravenously applied nanoparticles or gel. The columns represent the time after injection of the sample, whereas the rows quantify the time-dependent toxic effects. The brightness of the squares is proportional to the number of infected eggs.

Overall, we showed that the NP-gel concept represents a very suitable, non-toxic method for storage and manipulation with SiNP. The most significant findings of this study are: i) the morphological features and the critical, size-dependent properties of the nanomaterial that can be

often lost in solution after few minutes, are preserved in the responsive hydrogel for hours even when the particles were exposed to complex cell culture medium during storage; ii) the presented method is practical and the nanomaterial stored in the responsive hydrogel made by Fmoc-gal can be used in range of biologically relevant applications and tests; iii) the biocompatibility experiments indicated that the SiNP sample, including the individual gel components was non-toxic, despite the presence of gel fibres in the sample and finally, iv) the synthesis of the gelator, Fmoc-gal is industrially scalable, which could facilitate the translation of this method from the lab to a commercial product. We believe that the presented, proof-of-concept, gel-storage method represents a valuable alternative to the existing storage techniques and it will encourage scientists to accelerate research in the promising field of nanotechnology.

ASSOCIATED CONTENT

Supporting Information. The hydrogel storage concept was animated and it can be seen free of charge here: https://www.youtube.com/watch?v=EUQns52Q_q4&feature=em-share_video_user. Figure 3 represents static images taken from a video, which can be seen here: https://www.youtube.com/watch?v=EmAzEVbGbGE&feature=em-share_video_user.

AUTHOR INFORMATION

Corresponding Author

* Corresponding author: V.Gubala@kent.ac.uk

ACKNOWLEDGEMENT

Giorgia Giovannini would like to thank University of Kent for providing her PhD fellowship. Ondrej Stranik would like to thank Dr. Henkel for providing the microfluidic chip.

REFERENCES

Alkilany AM and Murphy CJ. 2010. Toxicity and cellular uptake of gold nanoparticles: what we have learned so far? J Nanopart Res 12:2313-2333.

Bae SW, Tan W and Hong J-I. 2012. Fluorescent dye-doped silica nanoparticles: new tools for bioapplications. Chem Commun 48:2270-2282.

Bagwe RP, Yang C, Hilliard LR and Tan W. 2004. Optimization of Dye-Doped Silica Nanoparticles Prepared Using a Reverse Microemulsion Method. Langmuir 20:8336-8342.

Bauer M, Lautenschlaeger C, Kempe K, Tauhardt L, Schubert US and Fischer D. 2012. Poly (2-ethyl-2-oxazoline) as Alternative for the Stealth Polymer Poly (ethylene glycol): Comparison of in vitro Cytotoxicity and Hemocompatibility. Macromol Bioscience 12:986-998.

Burns A, Sengupta P, Zedayko T, Baird B and Wiesner U. 2006. Core/Shell Fluorescent Silica Nanoparticles for Chemical Sensing: Towards Single-Particle Laboratories. Small 2:723-726.

Cascio C, Gilliland D, Rossi F, Calzolai L and Contado C. 2014. Critical Experimental Evaluation of Key Methods to Detect, Size and Quantify Nanoparticulate Silver. Anal Chem 86:12143-12151.

Emoto K, Van Alstine JM and Harris JM. 1998. Stability of Poly(ethylene glycol) Graft Coatings. Langmuir 14:2722-2729.

Fang C, Bhattarai N, Sun C and Zhang M. 2009. Functionalized Nanoparticles with Long-Term Stability in Biological Media. Small 5:1637-1641.

Gianoncelli A, Marmorato P, Ponti J, Pascolo L, Kaulich B, Uboldi C, Rossi F, Makovec D, Kiskinova M and Ceccone G. 2013. Interaction of magnetic nanoparticles with U87MG cells studied by synchrotron radiation X-ray fluorescence techniques. X-Ray Spectrometry 42:316-320.

Giovannini G, Kunc F, Piras CC, Stranik O, Edwards AA, Hall AJ and Gubala V. 2017. Stabilizing silica nanoparticles in hydrogels: impact on storage and polydispersity. RSC Advances 7:19924-19933.

Graf C, Gao Q, Schütz I, Noufele CN, Ruan W, Posselt U, Korotianskiy E, Nordmeyer D, Rancan F, Hadam S, Vogt A, Lademann J, Haucke V and Rühl E. 2012. Surface Functionalization of Silica Nanoparticles Supports Colloidal Stability in Physiological Media and Facilitates Internalization in Cells. Langmuir 28:7598-7613.

Gubala V, Crean C, Nooney R, Hearty S, McDonnell B, Heydon K, O'Kennedy R, MacCraith BD and Williams DE. 2011. Kinetics of immunoassays with particles as labels: effect of antibody coupling using dendrimers as linkers. Analyst 136:2533-2541.

Gubala V, Le Guevel X, Nooney R, Williams DE and MacCraith B. 2010. A comparison of mono and multivalent linkers and their effect on the colloidal stability of nanoparticle and immunoassays performance. Talanta 81:1833-1839.

Hamburger V and Hamilton HL. 1951. A series of normal stages in the development of the chick embryo. J Morphol 88:49-92.

Kho K and Hadinoto K. 2010. Aqueous re-dispersibility characterization of spray-dried hollow spherical silica nano-aggregates. Powder Technol 198:354-363.

Ma K, Mendoza C, Hanson M, Werner-Zwanziger U, Zwanziger J and Wiesner U. 2015. Control of Ultrasmall Sub-10 nm Ligand-Functionalized Fluorescent Core–Shell Silica Nanoparticle Growth in Water. Chem Mater 27:4119-4133.

Ma K, Sai H and Wiesner U. 2012. Ultrasmall Sub-10 nm Near-Infrared Fluorescent Mesoporous Silica Nanoparticles. J Am Chem Soc 134:13180-13183.

MacCuspie RI, Allen AJ and Hackley VA. 2011. Dispersion stabilization of silver nanoparticles in synthetic lung fluid studied under in situ conditions. Nanotoxicol 5:140-156.

Moore CJ, Giovannini G, Kunc F, Hall AJ and Gubala V. 2017. 'Overloading' fluorescent silica nanoparticles with dyes to improve biosensor performance. J Mater Chem B 5:5564-5572.

Moore CJ, Monton H, O'Kennedy R, Williams DE, Nogues C, Crean C and Gubala V. 2015. Controlling colloidal stability of silica nanoparticles during bioconjugation reactions with proteins and improving their longer-term stability, handling and storage. J Mater Chem B 3:2043-2055.

Müller R, Stranik O, Schlenk F, Werner S, Malsch D, Fischer D and Fritzsche W. 2015. Optical detection of nanoparticle agglomeration in a living system under the influence of a magnetic field. J Magn Magn Mater 380:61-65.

Nel AE, Madler L, Velegol D, Xia T, Hoek EMV, Somasundaran P, Klaessig F, Castranova V and Thompson M. 2009. Understanding biophysicochemical interactions at the nano-bio interface. Nat Mater 8:543-557.

O'Connell CL, Nooney R and McDonagh C. 2017. Cyanine5-doped silica nanoparticles as ultra-bright immunospecific labels for model circulating tumour cells in flow cytometry and microscopy. Biosens Bioelectron 91:190-198.

Orts-Gil G, Natte K, Drescher D, Bresch H, Mantion A, Kneipp J and Oesterle W. 2011. Characterisation of silica nanoparticles prior to in vitro studies: from primary particles to agglomerates. J Nanopart Res 13:1593-1604.

Park J-H, Gu L, von Maltzahn G, Ruoslahti E, Bhatia SN and Sailor MJ. 2009. Biodegradable luminescent porous silicon nanoparticles for in vivo applications. Nat Mater 8:331-336.

Park SJ, Kim YJ and Park SJ. 2008. Size-Dependent Shape Evolution of Silica Nanoparticles into Hollow Structures. Langmuir 24:12134-12137.

Peng M, Li H, Luo Z, Kong J, Wan Y, Zheng L, Zhang Q, Niu H, Vermorken A, Van de Ven W, Chen C, Zhang X, Li F, Guo L and Cui Y. 2015. Dextran-coated superparamagnetic nanoparticles as potential cancer drug carriers in vivo. Nanoscale 7:11155-11162.

Petersson K, Ilver D, Johansson C and Krozer A. 2006. Brownian motion of aggregating nanoparticles studied by photon correlation spectroscopy and measurements of dynamic magnetic properties. Anal Chim Acta 573:138-146.

Provis JL and Vlachos DG. 2006. Silica nanoparticle formation in the TPAOH-TEOS-H2O system: A population balance model. J Phys Chem B 110:3098-3108.

Rimer JD, Trofymluk O, Navrotsky A, Lobo RF and Vlachos DG. 2007. Kinetic and Thermodynamic Studies of Silica Nanoparticle Dissolution. Chem Mater 19:4189-4197.

Ruiz A, Hernandez Y, Cabal C, Gonzalez E, Veintemillas-Verdaguer S, Martinez E and Morales MP. 2013. Biodistribution and pharmacokinetics of uniform magnetite nanoparticles chemically modified with polyethylene glycol. Nanoscale 5:11400-11408.

Sánchez-Moreno P, Buzón P, Boulaiz H, Peula-García JM, Ortega-Vinuesa JL, Luque I, Salvati A and Marchal JA. 2015. Balancing the effect of corona on therapeutic efficacy and macrophage uptake of lipid nanocapsules. Biomater 61:266-278.

Schlenk F, Werner S, Rabel M, Jacobs F, Bergemann C, Clement JH and Fischer D. 2017. Comprehensive analysis of the in vitro and ex ovo hemocompatibility of surface engineered iron oxide nanoparticles for biomedical applications. Arch Toxicol:1-16.

Shaterabadi Z, Nabiyouni G and Soleymani M. 2017. High impact of in situ dextran coating on biocompatibility, stability and magnetic properties of iron oxide nanoparticles. Mater Sci Eng C 75:947-956.

Sokolov SV, Tschulik K, Batchelor-McAuley C, Jurkschat K and Compton RG. 2015. Reversible or Not? Distinguishing Agglomeration and Aggregation at the Nanoscale. Anal Chem 87:10033-10039.

Tivnan A, Orr WS, Gubala V, Nooney R, Williams DE, McDonagh C, Prenter S, Harvey H, Domingo-Fernandez R, Bray IM, Piskareva O, Ng CY, Lode HN, Davidoff AM and Stallings RL. 2012. Inhibition of Neuroblastoma Tumor Growth by Targeted Delivery of MicroRNA-34a Using Anti-Disialoganglioside GD(2) Coated Nanoparticles. Plos One 7 7:(5).

Tomaszewska E, Soliwoda K, Kadziola K, Tkacz-Szczesna B, Celichowski G, Cichomski M, Szmaja W and Grobelny J. 2013. Detection Limits of DLS and UV-Vis Spectroscopy in Characterization of Polydisperse Nanoparticles Colloids. J Nanomater 2013:10.

Venditto VJ and Szoka FC, Jr. 2013. Cancer nanomedicines: so many papers and so few drugs! Adv Drug Deliv Rev 65:80-88.

Wang EC and Wang AZ. 2014. Nanoparticles and their applications incell and molecular biology. Integr Biol 6:9-26.

Wang S, Xu T, Yang Y and Shao Z. 2015. Colloidal Stability of Silk Fibroin Nanoparticles Coated with Cationic Polymer for Effective Drug Delivery. Acs Appl Mater Inter 7:21254-21262.

Zaloga J, Janko C, Agarwal R, Nowak J, Müller R, Boccaccini A, Lee G, Odenbach S, Lyer S and Alexiou C. 2015. Different Storage Conditions Influence Biocompatibility and Physicochemical Properties of Iron Oxide Nanoparticles. Int J Mol Sci 16:9368.

Zaloga J, Janko C, Agarwal R, Nowak J, Muller R, Boccaccini AR, Lee G, Odenbach S, Lyer S and Alexiou C. 2015. Different Storage Conditions Influence Biocompatibility and Physicochemical Properties of Iron Oxide Nanoparticles. Int J Mol Sci 16:9368-9384.